Progr Colloid Polym Sci (1997) 103:268–279

M.M. Lipp
K.Y.C. Lee
J.A. Zasadzinski
A.J. Waring

Protein and lipid interactions in lung surfactant monolayers

Received: 12 December 1996
Accepted: 13 December 1996

M.M. Lipp · K.Y.C. Lee ·
Dr. J.A. Zasadzinski (✉)
Department of Chemical Engineering
University of California
Santa Barbara, California 93106-5090, USA

A.J. Waring
Department of Pediatrics
King/Drew University Medical Center and
Perinatal Laboratories
Harbor-UCLA School of Medicine
Los Angeles, California 90059, USA

Abstract Human lung surfactant protein SP-B and its amino terminus ($SP\text{-}B_{1\text{-}25}$) alter the phase behavior of palmitic acid (PA) monolayers by inhibiting the formation of condensed phases and creating a new fluid PA-protein phase. This fluid phase increases the compressibility of the monolayers by forming a network that separates condensed phase domains at coexistence and persists to high surface pressures. The network changes the monolayer collapse nucleation from a heterogeneous to a more homogeneous process through isolating individual condensed phase domains. This results in higher surface pressures at collapse, and monolayers easier to respread on expansion, factors essential to the in vivo function of lung surfactant. The network is stabilized by low line tension between the coexisting phases as confirmed by the formation of extended linear domains or "stripe" phases. Similar stripes are found in monolayers of fluorescein-labeled $SP\text{-}B_{1\text{-}25}$, suggesting that the reduction in line tension is due to the protein. Comparison of isotherm data and observed morphologies of monolayers containing $SP\text{-}B_{1\text{-}25}$ with those containing the full SP-B protein shows that the peptide retains most of the native activity of the protein, which may lead to cheaper and more effective synthetic replacement formulations.

Key words Langmuir trough – isotherms – fluorescence microscopy – Brewster angle microscopy

Introduction

Basic interfacial science and engineering principles can be applied to fundamental problems in biology to bring a new perspective to identifying the mechanisms of disease. Work in our laboratory has involved the study of lung surfactant monolayers. Lung surfactant (LS) is a complex mixture of lipids and proteins that lines the alveoli and allows the lungs to function properly [1]. LS consists primarily of the saturated phospholipid dipalmitoylphosphatidylcholine (DPPC), along with significant amounts of unsaturated and anionic phospholipids such as phosphatidylglycerols and lesser amounts of neutral lipids such as palmitic acid (PA) and cholesterol. LS also contains four proteins; two of these, termed SP-B and SP-C, are hydrophobic and surface active. LS works by both lowering the surface tension inside the lungs to reduce the work it takes to inhale and by stabilizing the lungs through varying the surface tension as a function of lung volume. To accomplish this, the LS mixture must adsorb rapidly from the type II cells lining the alveoli where LS is produced to the air/fluid interface of the alveoli. Once at the interface, LS must form a monolayer that can both achieve low surface tensions upon compression and vary the surface tension as a function of the alveolar radius. This monolayer must also be capable of respreading rapidly if it collapses due to over-compression during exhalation. A failure of this

system, either due to insufficient levels of LS or inactivation of existing LS can lead to respiratory distress syndrome (RDS), a potentially lethal disease in both adults and premature infants [2].

When RDS occurs, the lack of a properly functioning LS system results in a progressive failure of the lungs, which is manifested clinically by atelectasis (collapsed alveoli), decreased lung compliance (stiff lungs), decreased functional residual capacity (FRC, a measure of the amount of air left in the lungs after exhalation), systemic hypoxia (oxygen starvation), and lung edema (bleeding in the lungs) [3]. Neonatal RDS (nRDS) is known to be caused by a lack of sufficient surfactant levels (surfactant-deficient infants typically have less than 5 mg/kg of LS in their lungs, while typical healthy newborns have approximately 100 mg/kg). There are over 40000 cases of neonatal RDS diagnosed in the United States annually, resulting in thousands of deaths [3]. Additionally, nRDS has traditionally been very difficult and costly to treat, as affected infants require intensive care for extended periods. Up until 1989, the primary treatment method available for neonatal RDS has been forced lung ventilation [4]. However, the large ventilation pressures needed to overcome the high alveolar surface tension of nRDS infants often complicates matters by causing mechanical barotrauma. This ventilation-induced trauma can result in lung leakage and hemorrhaging, rupture and necrosis of lung tissues, injury of the epithelial cells lining the alveoli, and permanent damage to the lungs such as bronchopulmonary dysplasia (BPD, a chronic lung disease most likely due to ventilation-induced barotrauma and is characterized by excess CO_2 levels in the blood and hypoxia, as well as an abnormal lung morphology that persists long after birth) if the infant survives [4]. Lung hemorrhaging is particularly problematic, as soluble blood serum proteins such as albumin are believed to inactivate any LS present in the alveoli; this can result in a downward cycle wherein ventilation actually worsens the condition.

In 1989, the FDA approved two formulations for the treatment of neonatal RDS by surfactant replacement therapy (SRT), in which exogenous surfactant mixtures are administered directly into the lungs of affected infants [5]. The first of these, called Survanta, consists of an organic extract of bovine LS lipids and hydrophobic proteins supplemented with synthetic palmitic acid (PA) and tripalmitin. The second formulation, called Exosurf, contains DPPC combined with synthetic, nonbiological emulsifying lipids with no relation to natural LS. Administration of mixtures such as these to affected infants has been proven to be a very effective treatment method for nRDS [6]. Benefits of treatment include: improvement in systemic oxygenation, reduced need for ventilation, more uniformly inflated lungs, increased lung compliance, increased stability during deflation, and an increased FRC. The initiation of replacement therapies has coincided with a significant decline in the mortality rate of nRDS infants. SRT has been shown to reduce mortality rates by 30–50% for nRDS infants, and it has been estimated that 80% of the decline in the infant mortality rate of the United States between 1989 and 1990 could be attributed solely to the use of surfactant [6, 7]. SRT has also resulted in a significant savings for the treatment of nRDS infants. In a recent study examining the clinical effectiveness and financial ramifications of SRT, it was shown that inflation-adjusted charges per survivor declined by 10%, whereas the cost of care for each infant who died declined by over 30% after initiation of SRT, resulting in an estimated net saving of approximately $90 million per year [6].

However, further improvements in SRT formulations have been hindered by the lack of a fundamental understanding of how the LS system works and what the specific roles of each of the individual components are. Proposed replacement formulations can be divided into four classes: (i) natural LS extracts, (ii) modified LS extracts (natural extracts supplemented with synthetic lipids), (iii) synthetic formulations modeled on natural LS, and (iv) synthetic formulations with no relation to natural LS. Natural LS extracts have been shown to be effective both in vitro and in vivo, but human sources are limited, while animal sources are difficult and expensive to purify and pose the risk of containing viral or proteinaceous contaminants. For the case of modified LS extracts the same concerns exist, and although supplementing LS extracts with PA typically results in an improvement of activities the mechanism behind this improvement is unknown.

As with any natural product, both natural and modified LS extracts can have a wide variability in composition from batch to batch. These concerns have led to the study of synthetic LS formulations for which the composition can be better defined. Mixtures containing synthetic LS lipids with highly purified natural proteins such as SP-B and SP-C have been shown to be of comparable or better activity than many natural extracts; however a fundamental rationale for choosing the ratio of lipids to proteins for such mixtures besides their overall apparent activities in vivo is still lacking. Furthermore, LS proteins are difficult and expensive to obtain in a highly-purified form, and there does not yet exist a suitable host-vector system for the production of these proteins on a large scale through genetic engineering techniques (which is a common problem for surface-active proteins).

An ideal replacement formulation would be a mixture of synthetic lipids, in a ratio based on a good understanding of their individual functions in LS, combined with simple peptide sequences, produced via solid-state synthesis techniques, which capture the full activity of the

native LS mixture. Such a mixture could be easily and cheaply produced, and the composition could be tailored to optimize the properties of the mixture for the treatment of specific cases, ranging from rapid distribution and spreading for nRDS infants to an increased resistance to inactivation by serum proteins in barotrauma cases. Currently, SRT is not yet widely available in medical hospitals and centers around the United States [6]. Although the mortality rate for nRDS infants has been declining since the advent of successful surfactant replacement strategies, the incidence of low birth weight infants has been steadily rising [7]. The availability of standardized replacement formulations with a fully quantified mechanism of action could lead to a more widespread use of SRT to help save the lives of both infants and adults. The key to designing effective replacement formulations is a thorough understanding of the function and activity of each of the LS components.

Although it was known as early as 1929 that the surface tension in normal lungs was low [8], LS itself was not identified as a substance until 1959 by Avery and Mead [9]. Using a Langmuir trough, they demonstrated that DPPC was the key component for the surface tension lowering effect. It was also discovered that nRDS infants had significantly lower amounts of LS than normal infants. However, the administration of aerosolized DPPC directly into the lungs of nRDS infants was shown to have no beneficial effect whatsoever in most cases (due to its rigidity at physiological temperatures, DPPC does not spread well at the air/water interface; it also does not adsorb well to the air/water interface from solution), which indicated the importance of the non-DPPC components of LS [10]. Subsequent studies showed that whole LS obtained from mature animals could be used as an effective LS replacement in both premature animals and infants [11, 12]. Several in vitro and in vivo studies on both natural LS extracts and synthetic lipid mixtures demonstrated that the unsaturated and anionic lipids in LS as well as the proteins act to fluidize the DPPC-rich mixture, allowing it to adsorb rapidly to the air/fluid interface of the alveoli [13–16]. The fact that these fluidizing components are individually incapable of forming monolayers that can attain low surface tensions has led to the hypothesis that these components are "squeezed-out" of the LS monolayer, leaving it enriched in DPPC [17–19]. However, removal of all of these fluidizing components would prevent the DPPC-enriched LS monolayer from respreading rapidly upon the event of collapse. Moreover, it has been shown that the presence of LS proteins in pre-formed monolayers of DPPC greatly enhances the rate of adsorption of new materials to the interface [20]. A systematic study of monolayers of unsaturated or anionic LS lipids containing surface-active LS proteins can help in the understanding of the LS system, as well as determine the mechanism by which additives such as PA enhance the activity of LS extracts.

Our recent work has centered on the elucidation of the roles of both PA and SP-B protein in both the natural LS system and in replacement surfactant formulations. As a large percentage of the fluidizing LS lipids are anionic, while the surface-active LS proteins such as SP-B have a net positive charge, it is plausible that these components may interact synergistically in LS monolayers to increase their surface activity. Although PA has been shown to greatly improve the activity of replacement formulations, the mechanism of action of this component is still not understood [14, 21]. While the phase behavior of pure PA is well known, it does not indicate how PA "improves" the properties of LS mixtures. It has been postulated that PA may interact selectively with SP-B in LS monolayers, resulting in the retention of both components in the monolayer up to collapse. This would possibly allow these components to perform such functions as enhancing the respreading rate of material from the collapsed phase, as well as increasing the rate of adsorption and incorporation of material from the subphase. The study of mixed PA/SP-B monolayers will reveal the presence of any synergistic interactions between these components and may help explain how these components function in the whole LS monolayer.

Protein engineering can also be used to relate the amino acid sequence of SP-B protein to its activity in LS. Due to the current lack of a suitable expression system for the production of SP-B and the significant cost of synthesizing the native protein on the scales needed to treat RDS, work in our lab has focused on attempting to figure out what is the key functional moiety of the protein in the hopes of developing simpler sequences for replacement formulations. We have found that a 25 amino acid long sequence based on the amino-terminus of native SP-B possesses similar activity as that of the native protein both in vitro and in vivo [22, 23]. It appears that the key to the activity of both the full-length and the shortened sequence is the presence of an amphipathic alpha helix with the positively charged residues aligned on one side of the helix and the hydrophobic residues on the other [24].

The goal of our work is to determine the specific mechanism of action of both PA and SP-B in LS. Using the information obtained from the study of simple binary mixtures, we hope to form a basis for the study of a complete synthetic LS mixture. While this is a common approach to studying multicomponent phase diagrams in chemical engineering and materials science, it is surprisingly uncommon in biology and medicine. Quite often, the number of components in a biological system is so large that this approach is impossible. However, LS is

a relatively simple mixture and lends itself to a systematic approach. We have utilized direct monolayer imaging techniques such as fluorescence, polarized fluorescence, and Brewster angle microscopies to study the phase behavior and collapse mechanics of mixed PA and SP-B monolayers. We have discovered that synergistic interactions between SP-B and PA remove the driving force for squeeze-out of either component from LS monolayers, and explain how respreading of the post-collapse monolayer is facilitated. We have also manipulated the protein through the systematic introduction of point mutations to examine the effects of altering the hydrophobic/charge balance of the protein. This information can hopefully aid the rational design of synthetic LS formulations and the creation of simpler and cheaper peptide sequences to replace native LS proteins.

Experimental: visualizing lipid/protein monolayers

To study model LS monolayers, we have designed an integrated fluorescence, polarized fluorescence, and Brewster angle microscope/Langmuir trough assembly (an overview of this system is displayed in Fig. 1). Langmuir troughs have been used for the past 70 years to obtain surface tension vs. area isotherms of surfactant monolayers at the air/water interface. Surfactant monolayers can exist in several 2D phases as a function of the lateral density; at very high areas per molecule monolayers exist in a gas-like state, while monolayers with low areas per molecule exist in liquid-crystalline and solid phases. Unfortunately, isotherms can only provide macroscopic information concerning the phase state of the monolayer, the details of the nucleation and coexistence phenomena of the phase transitions cannot be determined (however, just as in 3D gases and liquids, a good understanding of the phase diagram is a necessary first step).

Several techniques have been developed over the last 15 years to visually probe the morphology of surfactant monolayers at the air–water interface. In fluorescence microscopy, a small amount of fluorescently labeled surfactant molecules is added to a monolayer; due to steric effects these tagged molecules tend to partition into less-ordered phases, which results in a visual contrast between coexisting phases [25–29]. Fluorescence microscopy has been used to determine domain sizes and shapes during phase transitions [25, 28, 30]. Polarized fluorescence microscopy (PFM) provides additional information on the lipid hydrocarbon chain ordering within condensed monolayers, especially in areas where the lipid hydrocarbon chains are tilted with respect to the surface normal [31, 32]. The interaction of the electric field vector of the polarized light with the absorption dipole moment of the fluorophore is dependent on the relative orientation of the molecule, hence using a polarized light source incident on the monolayer at an oblique angle as the excitation source allows for the detection of regions of different tilt directions.

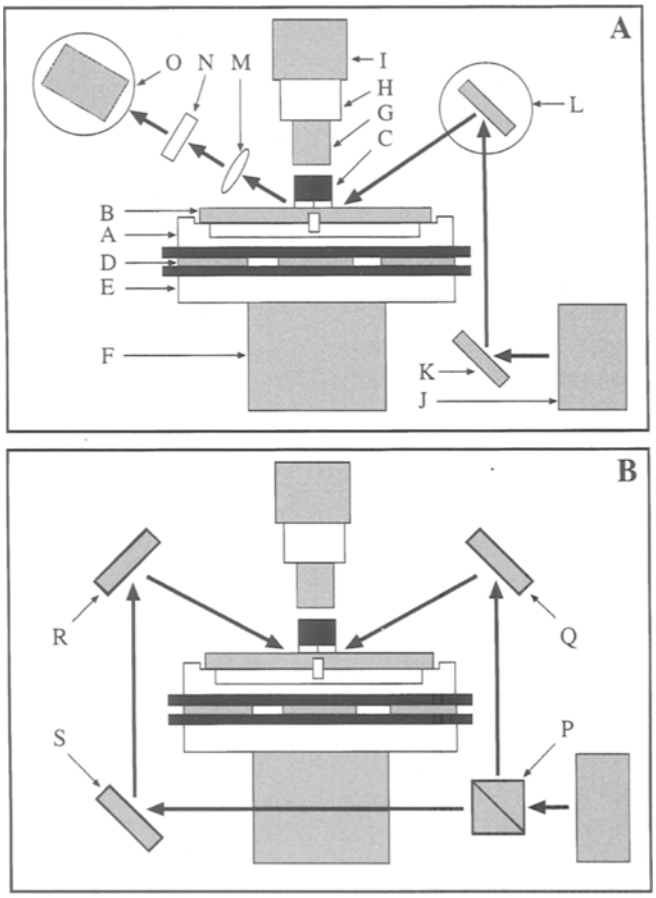

Fig. 1 A schematic of the FM/PFM/BAM assembly. **(A)** Configuration for dual FM/BAM operation. The labeled parts are: (A) Langmuir trough, (B) barrier, (C) surface pressure sensor, (D) thermoelectric elements, (E) water bath, (F) motorized *xyz* translation stage, (G) microscope objective, (H) mercury lamp/fluorescence filter cube assembly, (I) SIT camera, (J) laser, (K) mirror, (L) rotatable mirror, (M) lens, (N) polarizer cube (analyzer), (O) CCD camera (mounted on a rotatable stage). **(B)** Configuration for PFM operation. The parts specific to the PFM are (including the laser): (P) beam-splitter cube, (Q,R,S) mirrors. The bold arrows in both drawings denote the light path of the laser beam in the BAM and PFM modes. For the PFM mode, switching between the two beams shown in **(B)** from the beam-splitter rotates the plane of incidence of the beam with the surface by 180° and results in a reversal of contrast for regions of differing tilt directions in monolayers

A third optical microscopy technique, called Brewster angle microscopy (BAM), has only recently been developed [33, 34]. The benefits of BAM are that is provides information similar to fluorescence and polarized fluorescence microscopies without requiring the addition of

fluorescent probes. A p-polarized light beam is weakly reflected by a monolayer when the surface is illuminated at the Brewster angle (about 53° from the surface normal for the air/water interface). The intensity of the reflected light is a function of the local state of the monolayer; variations in the refractive index of the monolayer result in image contrast due to different reflected intensities. Allowing for the study of these monolayers without the presence of fluorescently labeled molecules, BAM confirms that the fluorescent probe molecules at low mole percentages do not influence the phase behavior seen via FM and PFM, and provides additional information on local tilt and other anisotropic orientational effects. However, little fluorescence or Brewster angle microscopy has been done on lung surfactants, especially on monolayers containing LS-specific proteins. The combined FM, PFM, and BAM assembly provides an ideal system for examining the mechanism of action between PA and SP-B protein, as well as the monolayer phase behavior and morphology of other mixed lipid and protein systems.

Single-component monolayers have a triple point temperature similar to 3D fluids that dictates the nature of phase transitions. Below the triple point, the gas phase transforms into what is called a liquid-condensed (l.c.) phase, analogous to the reverse of a solid to gaseous sublimation process for 3D systems. In the l.c. phase, the molecules are aligned at the interface with their tails extended towards the air, however they do not yet possess any long-range positional order and the hydrocarbon chains are relatively disordered (although they can possess long-range orientational order, forming tilted phases with a uniform tilt direction over macroscopic dimensions). The terminus of the gas–l.c. transition is exhibited in the isotherm by a sharp increase in surface pressure upon compression, termed the lift-off point, which corresponds to the disappearance of the gas phase. Above the triple point, the gas phase transforms into a 2D liquid-like phase, termed a liquid-expanded (l.e.) or fluid phase. In this "fluid-like" phase, the molecules are randomly arrayed and free to diffuse, and the hydrocarbon chains are in the liquid state. This fluid phase has a much higher compressibility relative change in area per change in surface pressure (i.e. $-(-1/A)(\partial A/\partial \Pi)_T$) than the l.c. phase, as evidenced by a decreased absolute value of the slope in the isotherm. Under further compression, this fluid phase undergoes a first-order transition into the l.c. phase, seen by the appearance of a plateau in the isotherm (there is an equivalent of the Gibbs phase rule in two-dimensions which states that first-order transitions in single-component monolayers should occur at a constant surface pressure, although this postulate has been greatly debated).

At elevated pressures both below and above the triple point, the l.c. phase undergoes a second-order phase transition (indicated by a kink point in the isotherm) into a solid-like phase, referred to as either solid-condensed (s.c.) or crystalline depending on the degree of order of the hydrocarbon chains. In these phases, the molecules are close-packed and aligned in a lattice, possessing quasi-long range positional order. Compressing the monolayer below the minimum area per surfactant molecule in the crystalline state results in the collapse of the monolayer and formation of a 3D phase either above or below the monolayer. Although the formation of 3D phases may be favored under equilibrium conditions for monolayers at relatively low pressures, there typically exists a substantial energy barrier for the collapse process to occur. This makes collapse a kinetically driven process that requires the input of an activation energy, and depends on such factors as the rate of compression of the monolayer. The ability to resist collapse determines the maximum pressure (or minimum surface tension) a monolayer may achieve. Monolayers which require higher activation energies to initiate collapse can attain and maintain higher surface pressures than those requiring lower activation energies. This leads to lower ultimate surface tensions, and these monolayers are "better" lung surfactants.

Considering the reverse process, the structure and location of the collapsed phase and the reversibility of the collapse process determines whether the collapsed phase will reincorporate itself upon re-expansion of the monolayer. Monolayers that are more resistant to collapse (and can achieve high surface pressures) usually do not respread well; collapse is an irreversible process in these systems and the collapsed phase remains in a bulk 3D state at the interface or is lost into the subphase. For proper functioning, ideal LS monolayers should resist collapse (and thus achieve low surface tensions) yet respread rapidly and completely (which seems to be a dichotomy in behavior and is incompatible with single-component monolayers).

We have found that the addition of SP-B protein results in a drastic alteration of the phase behavior of PA monolayers [35]. The presence of protein fluidizes PA monolayers under all experimental conditions. Although Langmuir isotherms show changes in phase behavior of PA due to the presence of protein, they do not reveal the mechanisms by which the protein effects these changes. Similar changes in both the compressibility and collapse pressure of monolayers have been observed in mixed fatty acid and polycationic polymer systems [36]. This suggests that these effects may be more general in nature, and provides additional motivation for studying simpler peptide sequences for replacement formulations. Direct visualization of the phase transitions and collapse processes occurring in mixed PA/SP-B monolayers allows us to relate monolayer morphology to isotherm data which

helps us to elucidate the mechanisms behind this phenomenon.

Fluorescence microscopy of PA/SP-B_{1-25} monolayers

Upon deposition of pure PA at an area per molecule of approximately 60 Å^2 on a pure water subphase at 16°C, the monolayer exists in a gas–l.c. coexistence region. As shown in Fig. 2A, this is seen as a coexistence of circular light gray l.c. domains in a dark gaseous background (the probe used in this study, NBD-HDA, quenches when it comes into contact with the subphase, making the gas phase appear dark). At the liftoff point, the monolayer is entirely in the l.c. phase, as seen by a lack of contrast in the monolayer (Fig. 2B). Upon further compression, the monolayer transforms from the l.c. phase into a solid phase of homogeneous contrast. When 20 wt% SP-B_{1-25} is added to these PA monolayers, a new bright fluid phase can be seen to form (in addition to the gas and l.c. phases) at high areas per molecule. This fluid phase persists past the liftoff point, forming a network that partitions the PA-rich l.c. phase into small, circular domains (Fig. 2C). The network persists through the solid phase transition, segregating the solid domains prior to collapse.

We observed a similar trend at temperatures above the triple point of PA on a pure water subphase. At such temperatures, pure PA monolayers exist as a homogeneous bright fluid phase at the liftoff point. Upon compression, the monolayers proceed through a first-order fluid to l.c. transition, evidenced by the formation of a plateau region in the isotherm. During this transition, the l.c. phase can be seen to nucleate from the bright fluid phase background and grow into large, dark, circular l.c. domains (Fig. 2D). These domains eventually pack together at high pressures, leading to the disappearance of the l.e. phase and the formation of a homogeneous sheet of l.c. phase. This l.c. phase again transforms into a homogeneous solid phase at low areas per molecule (Fig. 2E). The addition of SP-B can be seen to greatly affect the fluid to l.c. phase transition. The protein decreases the size and increases the nucleation density of the l.c. phase (Fig. 2F). This again results in a partitioning of the l.c. phase into small, circular domains as seen at lower temperatures. In the presence of protein, the bright fluid phase remains upon transition of the l.c. phase into the solid phase and persists to high surface pressures.

We have discovered that this partitioning of the condensed phase domains by the protein-induced network has a drastic effect on the collapse processes occurring in these monolayers. For pure PA monolayers on a pure water subphase, compressing past the limiting area per molecule in the crystalline state results in the collapse of the monolayer and the formation of 3D bulk phases. As seen in Figs. 3A and C, both below and above the triple point, collapse occurs heterogeneously at isolated points across the monolayer and results in the formation of large, rigid, dendritic-like collapsed-phase domains. This process is

Fig. 2 Fluorescence images of PA and PA/SP- B_{1-25} films containing 0.5 mol% NBD-HDA on a pure water subphase. (A–C) Images taken at 16°C of (A) a pure PA film in the l.c.-g coexistence region (the l.c. domains are light gray, the gas phase is black), (B) the same film at the liftoff point, consisting entirely of l.c. phase, and (C) a PA/20 wt% SP-B_{1-25} at the liftoff point, showing the existence of a new, bright fluid phase which breaks up the l.c. domains. (D–F) Images taken at 28°C of (D) a pure PA film in the fluid-condensed coexistence region (area per PA molecule 35 Å^2), (E) upon further compression of the same film into the solid phase, and (F) a PA/20 wt% SP-B_{1-25} film in the fluid-condensed coexistence region (area per PA molecule 35 Å^2), showing a decreased size and increased nucleation density of the condensed domains

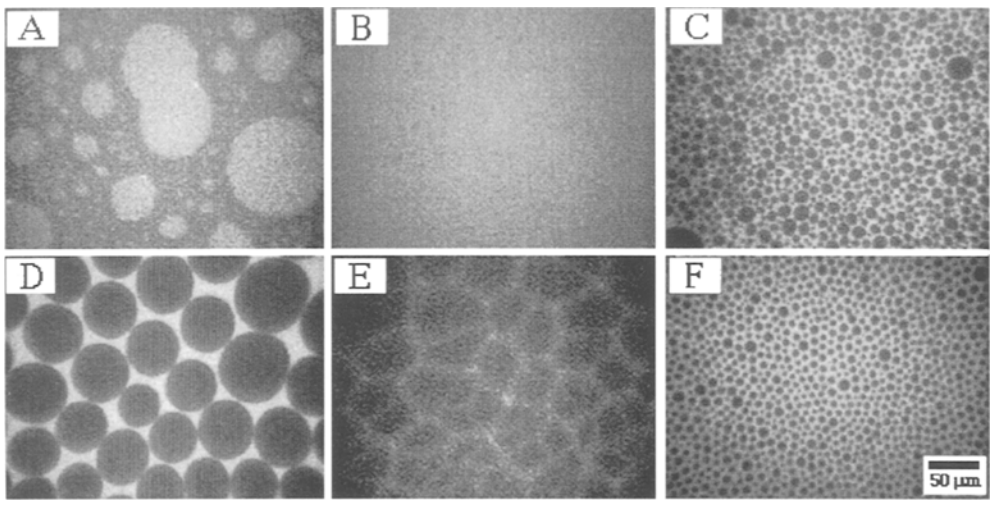

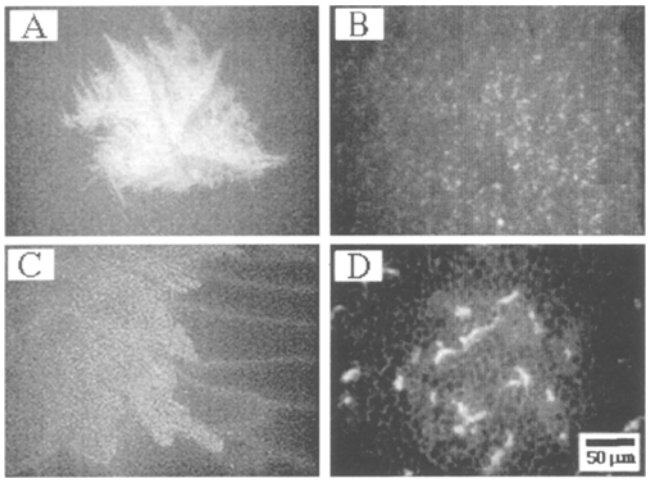

Fig. 3 Fluorescence images of the collapse behavior of PA and PA/SP-B_{1-25} monolayers containing 0.5 mol% NBD-HDA on a pure water subphase. (A, B) Images taken at 16°C of the collapsed phase domains for (A) pure PA and (B) PA/20 wt% SP-B_{1-25}. (C, D) Images taken at 28°C of the collapsed phase domains for (C) pure PA monolayer and (D) PA/20 wt% SP-B_{1-25}

very irreversible, with subsequent expansion and recompression of the monolayer resulting in a large hysteresis, which implies a loss of material from the surface. The presence of the protein network prevents the heterogeneous nucleation process from occurring; each partitioned domain must now nucleate collapse independently and homogeneously. This requires a larger activation energy, which results in a rise in the collapse pressure over that of pure PA. This phenomenon is the two dimensional analog of the classic experiments of Turnbull, who showed that many simple metallic liquids could be undercooled far below their thermodynamic freezing points [37]. By subdividing the liquid into micron-size droplets, Turnbull was able to reduce the likelihood of heterogeneous nuclei in a given droplet, leading to homogeneous nucleation at large undercooling. Similar effects have been observed for supercooling water in emulsion droplets, polymer gels, or porous media [38, 39]. Additionally, since collapse must occur independently in each domain, the resulting collapsed phase domains are significantly smaller and more evenly distributed (Fig. 3B and D), which makes the collapse event more reversible and facilitates the reincorporation of this phase into the monolayer upon re-expansion.

Although the phase behavior of PA is altered for monolayers on physiological, buffered saline subphases (pH = 6.9, 0.15 M NaCl), the presence of SP-B protein has similar effects to those seen on a pure water subphase. For pure PA monolayers, the buffered saline subphase conditions result in a change in the mechanism of collapse. The ionization of the headgroups inhibits the formation of bulk collapsed phases above the monolayer, where the electrostatic repulsion would be high. As a result, PA monolayers require a higher pressure to nucleate collapse, and collapse occurs via a bulk fracturing mechanism in which the monolayer cracks cooperatively over large length scales (Fig. 4A). This process is also irreversible, with the fractures persisting upon expansion. Below the triple point, the addition of SP-B protein again leads to the formation of a bright fluid phase which breaks up and partitions the condensed phase domains (Fig. 4B). In the presence of protein, the collapse mechanism shifts to a more homogeneous process. This network prevents the fracture event from occurring and shifts the mechanism to a nucleation and growth process, resulting in the appearance of a uniform distribution of small collapsed phase domains across the film (Fig. 4C).

Above the triple point on a buffered saline subphase, PA again undergoes a first-order fluid to l.c. transition, although the l.c. domains are smaller and more numerous due to the higher electrostatic repulsion within the l.c. phase nuclei (Fig. 4D). Domain shapes at a particular point of compression of a monolayer usually result from a balance between electrostatic repulsion and line tension; electrostatic repulsion favors the elongation of domains of the more condensed phase due to their higher lateral density, while line tension favors circular domains which minimize the perimeter. This balance most likely also has an influence on the size of the nuclei in monolayers undergoing a phase transition; the high electrostatic density in charged monolayers results in a smaller critical radius for the nuclei (with a corresponding increase in the required supersaturation pressure, assuming the line tension remains unchanged). However, upon further compression, the l.c. domains are actually seen to fuse together (Fig. 4E), eventually forming a contiguous sheet of l.c. phase prior to the solid transition which fractures upon collapse (Fig. 4F). The presence of protein reduces the size and increases the nucleation density of the l.c. domains at the fluid to l.c. transition (Fig. 4G). Upon further compression, the l.c. domains undergo limited fusion (Fig. 4H), however the size of the fused domains remains small and a bright phase network again persists right up to collapse. Collapse occurs via a homogeneous nucleation and growth mechanism at elevated pressures (Fig. 4I). For all cases, the increase in collapse pressure and the ease of the respreadability of the collapsed phase has important implications on the functioning of LS monolayers, effectively removing the driving force for the squeeze-out of components with low individual collapse pressures from LS monolayers and facilitating the respreading of the LS monolayer.

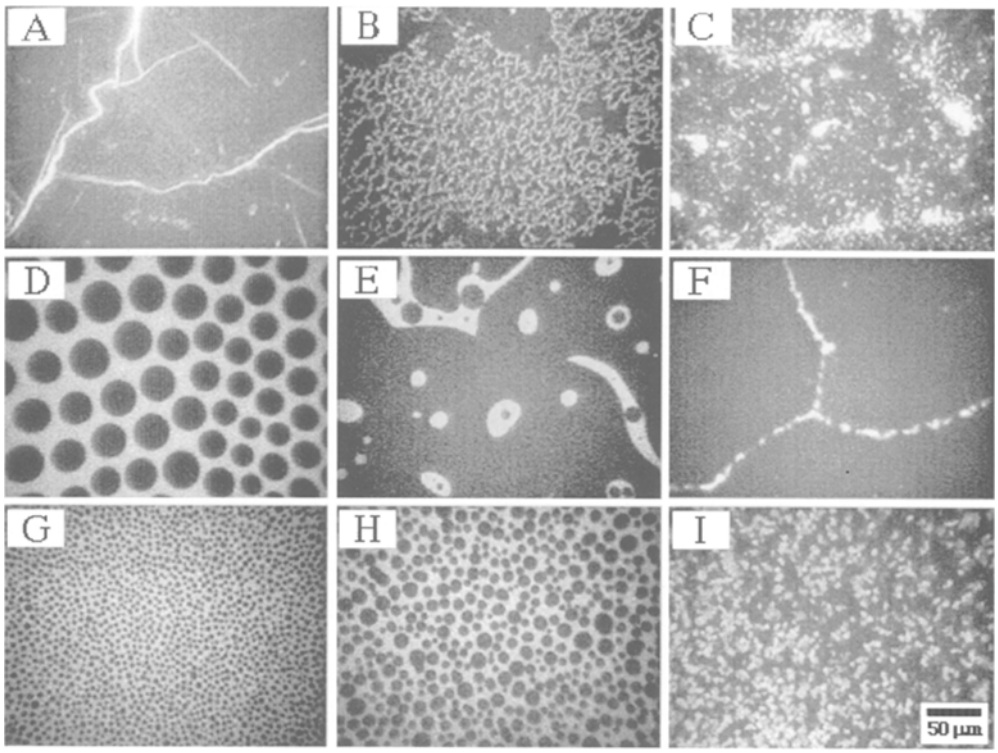

Fig. 4 Fluorescence images of PA/SP-B_{1-25} films containing 0.5 mol% NBD-HDA on a buffered saline subphase. (A–C) Fluorescence images at 16°C of (A) bulk fracturing collapse of a pure PA monolayer, (B) existence of a protein-rich bright phase network at elevated pressures of a PA/20 wt% SP-B_{1-25} monolayer, and (C) collapse of the same monolayer via a homogeneous nucleation and growth mechanism. (D–F) Images of a pure PA film at 25°C in (D) the fluid-condensed coexistence region, (E) after fusion of individual domains into a sheet of condensed phase upon further compression, and (F) the post-collapse fracturing of the film. (G–I) Images of a PA/20 wt% SP-B_{1-25} film at 25°C (G) in the fluid-condensed coexistence region (area per PA molecule 35 $Å^2$) (H) after limited fusion of the condensed domains, and (I) post-collapse, showing the nucleation and growth of small collapsed phase domains

The use of fluorescently labeled protein allows us to further investigate the specific mechanisms by which the protein alters the phase behavior of PA. In all cases shown so far, the formation of a bright phase network surrounding the small condensed phase domains results in the existence of a large amount of line interface between the phases. In analogy to the interfacial tension that exists between two bulk 3D phases, there exists a line tension between coexisting phases in two dimensions. If the line tension between two phases is high, there would be a large energetic cost upon increasing the perimeter between the phases while maintaining a constant area ratio between the phases. However, for this system it appears that the increase in perimeter between the fluid and condensed phases is allowed to occur due to the fact that the protein acts to lower the line tension between these phases. Direct evidence of this is obtained on buffered saline subphases at low temperatures and high areas per molecule, in which case stripe phases are formed in monolayers of PA/20 wt% SP-B (Fig. 5A). The formation of stripe phases in the presence of protein indicates a low line tension between the coexisting phases in these films (for coexisting domains in Langmuir monolayers, the characteristic width of a domain possessing an increased electrostatic density with respect to its surroundings scales as $\exp(\lambda/\mu^2)$, where λ is the line tension and μ is the difference in dipole density

Fig. 5 Fluorescence images of stripe phases and partitioning characteristics of SP-B_{1-25} and F-SP-B_{1-25} in PA monolayers. (A) A monolayer of PA/20 wt% SP-B_{1-25} on a buffered saline subphase at an area per PA molecule of 63 $Å^2$ showing the existence of stripe domains. (B) An image of a fluorescein–SP-B_{1-25} (F–SP-B_{1-25}) monolayer on a pure water suhphase at 23°C showing the formation of a "stripe" phase at low surface pressures. (C, D) Images of a monolayer of PA/20 wt% F–SP-B_{1-25} also containing 0.5 mol% Texas-red DPPE on a pure water subphase at 28°C showing the fluorescence from (C) the lipid probe and (D) the fluorescently labeled protein

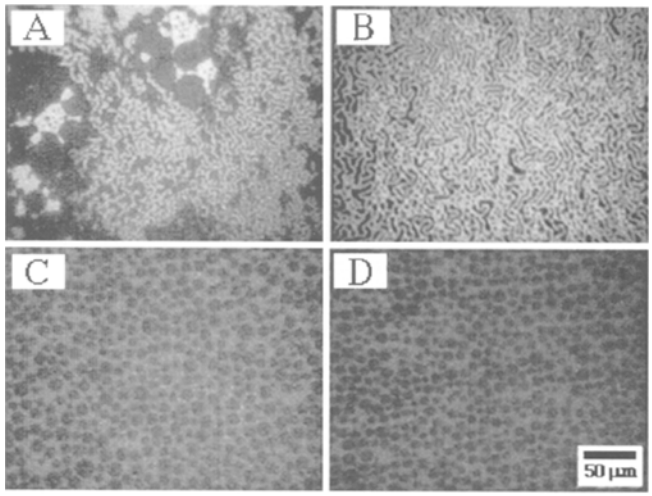

between the phases; stripe phases can occur when either λ is very small or μ is very large). Similar stripe phases are seen in pure films of fluorescein-labeled SP-B, which indicates that the low line tension is a direct effect of the presence of the protein (Fig. 5B). Using fluorescently labeled SP-B also allows us to pinpoint the location of the protein in the mixed films. A dual-probe experiment, in which both a lipid probe and SP-B protein labeled with a fluorescent tag emitting at different wavelengths are used, allows us to see which phase the protein tends to partition into during phase transitions. Rapidly switching between two filter cubes specific to each of the fluorophores in the film allows us to see the fluorescence from both the lipid phases and the protein at the same location. In all cases, the protein is seen to partition preferentially into the bright fluid phase (Figs. 5C and D).

Polarized fluorescence microscopy of PA/SP-B_{1-25} monolayers

PFM gives us additional information on the collapse behavior of these monolayers. As previously described, for condensed lipid phases in which the molecules are tilted in a specific direction with respect to the surface normal, the use of polarized light as the fluorescence excitation source results in contrast between regions of different tilt directions. PFM allows us to determine the influence of lipid molecule tilt on both the nature of the nucleation of collapse and the lack of reincorporation of the collapsed phase upon re-expansion. For pure PA monolayers at 16°C, the l.c. phase consists of domains of differing tilt directions bordering at defect lines and points (Fig. 6A). If these defect points are not allowed to anneal out when the film transforms to the untilted solid phase prior to collapse, they may act as heterogeneous nucleation sites and allow collapse to occur at lower pressures. In the presence of protein, the condensed phases are individually either untilted or of uniform tilt (Fig. 6C). This removes the influence of any tilt defects on the collapse nucleation process and requires each domain to nucleate collapse homogeneously. Furthermore, PFM reveals that the collapsed phase itself is tilted, while the underlying monolayer is untilted (Fig. 6B). This means that the collapsed phase is at a lower packing density with respect to the monolayer, and would have to contract in order to be reincorporated into the monolayer upon expansion, which may explain why these domains do not readily reincorporate into the monolayer upon re-expansion. For the protein-containing films, the collapsed phase domains themselves do not appear to be tilted (Fig. 6D), which in combination with their smaller sizes may ease their reincorporation into the monolayer. A similar process occurs at temperatures above the triple point; the large collapsed phase domains

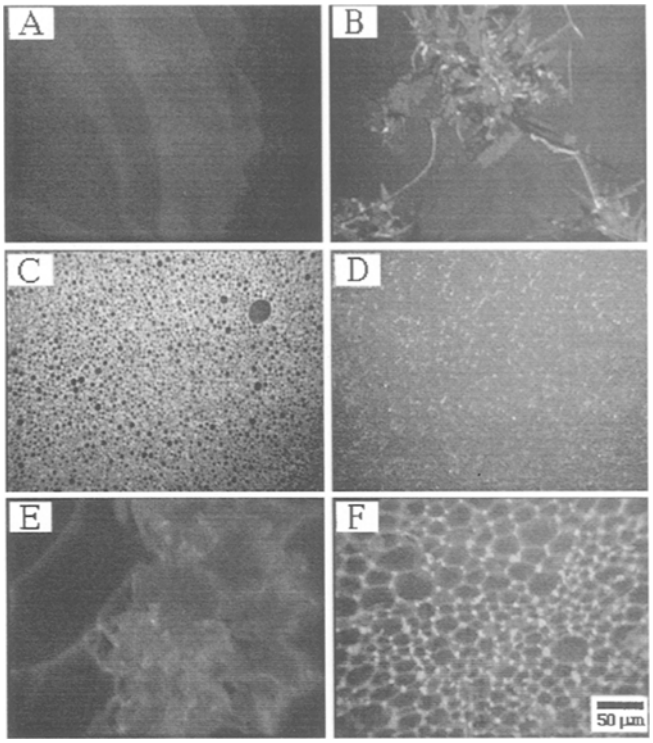

Fig. 6 Polarized fluorescence images of the collapse behavior of PA and PA/SP-B_{1-25} monolayers containing 0.5 mol% NBD-HDA. (A, B) Polarized fluorescence images of a PA film on a pure water subphase at 16°C (A) at a pressure of 15 mN/m in the liquid-condensed phase (with contrast resulting from domains of differing tilt direction), and (B) after collapse of the monolayer, showing the growth of a tilted collapsed phase domain. (C, D) Polarized fluorescence images of a PA/20 wt% SP-B_{1-25} film on a pure water subphase at 16°C (C) at a pressure of 15 mN/m (showing a lack of tilt contrast within the small condensed domains), and (D) after collapse of the monolayer, showing the homogeneous distribution of small collapsed phase domains. (E, F) Polarized fluorescence images of collapsed phase domains for films on a pure water subphase at 28°C for (E) pure PA and (F) PA/20 wt% SP-B_{1-25}

for pure PA are again tilted (Fig. 6E), while in the presence of 20 wt% SP-B_{1-25} the collapsed phase domains are smaller and do not grow past the boundaries of the original solid phase domains (Fig. 6F).

Brewster angle microscopy of PA/SP-B_{1-25} monolayers

A significant concern with the use of fluorescence and polarized fluorescence microscopies for the study of surfactant monolayers has been the possibility of artifacts due to the addition of foreign probe molecules to the system. BAM provides equivalent information to PFM without requiring the addition of a foreign probe molecule. Thus, we have used BAM to confirm that the probe molecules, present at low concentrations, do not influence the

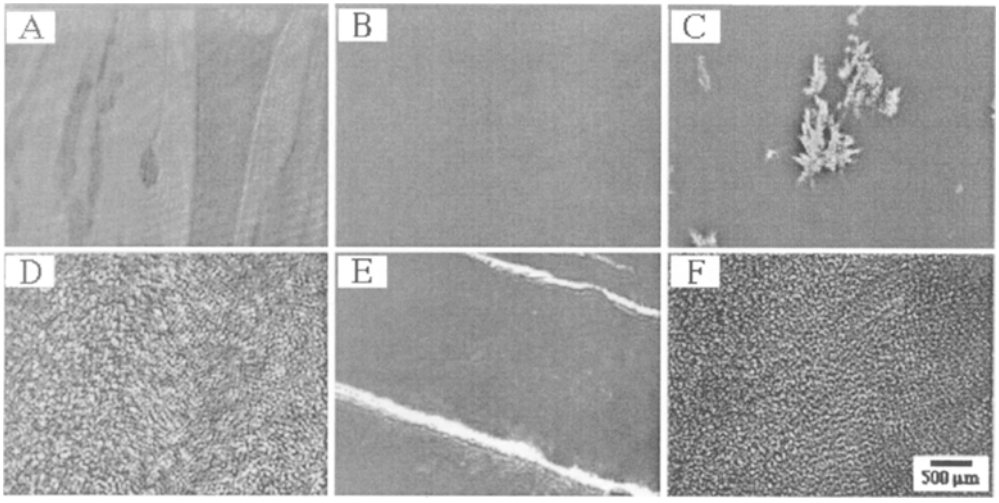

Fig. 7 Brewster angle microscope images of the collapse behavior of PA and PA/SP-B_{1-25} monolayers. (A–C) Brewster angle microscope images of a film of pure PA on a pure water subphase at 16°C (A) in the l.c. phase (with contrast arising from the existence of domains of differing tilt direction), (B) upon transition to the solid phase (showing the loss of tilt contrast), and (C) post-collapse (showing the presence of tilt contrast within the collapsed phase domain). (D) Brewster angle microscope image of a PA/20 wt% SP-B_{1-25} film on a pure water subphase at 16°C showing the growth of the uniform collapsed phase. (E, F) Images from monolayers on buffered saline subphases at 16°C showing (E) bulk fracture of a PA monolayer and (F) nucleation and growth of a collapsed phase for a PA/20 wt% SP-B_{1-25} film

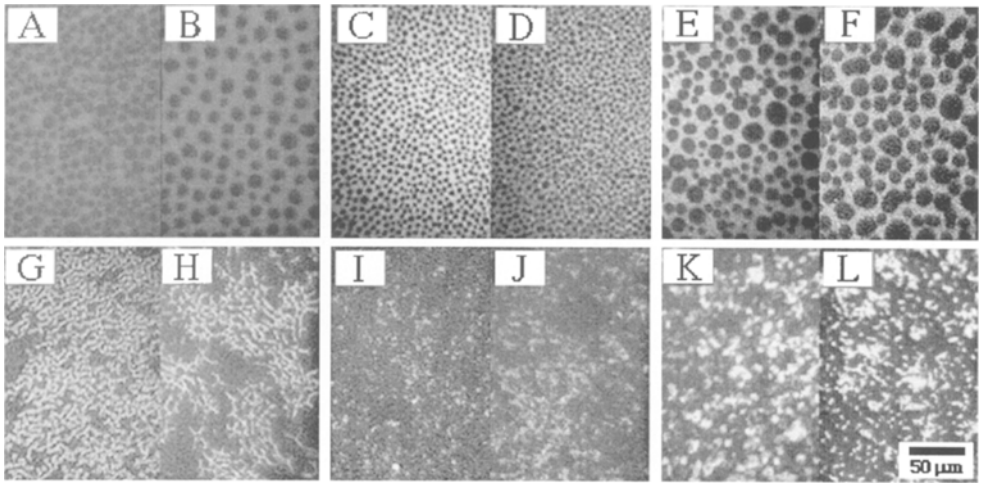

Fig. 8 Comparison of PA films containing SP-B_{1-25} and SP-B_{1-78} (also containing 0.5 mol% NBD-HDA) under various experimental conditions. (A, B) Fluorescence images of PA/SP-B films on a pure water subphase at 28°C in the l.e.–l.c. coexistence region containing (A) 20 wt% SP-B_{1-25} and (B) 20 wt% SP-B_{1-78}. (C, D) Fluorescence images on a buffered saline (0.15 M NaCl, pH = 6.9) subphase at 25°C in the fluid-condensed coexistence region containing (C) 20 wt% SP-B_{1-25} and (D) 20 wt% SP-B_{1-78}. (E, F) Fluorescence images of limited fusion of lc domains PA/SP-B films on a buffered saline (0.15 M NaCl, pH = 6.9) subphase at 25°C in the fluid-condensed coexistence region containing (E) 20 wt% SP-B_{1-25} and (F) 20 wt% SP-B_{1-78}. (G, H) Fluorescence images of stripe phases occurring in PA/SP-B films on a buffered saline subphase at 16°C containing (G) 20 wt% SP-B_{1-25} and (H) 20 wt% SP-B_{1-78}. (I, J) Fluorescence images of collapsed phase domains occurring in PA/SP-B films on a pure water subphase at 16°C containing (I) 20 wt% SP-B_{1-25} and (J) 20 wt% SP-B_{1-78}. (K, L) Images of PA/SP-B films post-collapse on a buffered saline subphase at 25°C containing (K) 20 wt% SP-B_{1-25} and (L) 20 wt% SP-B_{1-78}

morphologies observed in lipid/protein films via fluorescence and polarized fluorescence microscopies, and also to obtain images at larger length scales. In all cases so far in our laboratory, BAM has provided completely analogous images of monolayers of various components of LS to those obtained with fluorescence and PFM. This confirmation is of particular importance for the study of collapse of PA/SP-B_{1-25} films; sites of accumulation of

fluorescently labeled molecules could potentially act as heterogeneous nucleation sites. However, at all experimental conditions, BAM images of collapse show a similar shift in collapse mechanism as seen with fluorescence and polarized fluorescence microscopies. On pure water subphases, BAM images show the presence of tilt in the l.c. phase (Fig. 7A), the disappearance of this tilt contrast on transition to the solid phase (Fig. 7B), and the growth of large, isolated, tilted collapsed phase domains for pure PA films (Fig. 7C). On buffered saline subphases, BAM images further reveal the macroscopic dimensions of the fracture cracks in collapsed films of pure PA (Fig. 7E). For both subphases, in the presence of SP-B_{1-25}, BAM images show the homogeneous and uniform nature of the growth of the collapsed phase domains at a much higher nucleation density (Figs. 7D and F).

Comparison of SP-B_{1-25} to full-length SP-B protein

Earlier isotherm data obtained in our laboratory indicated that the amino-terminal segment of SP-B possesses most of the activity of the full-length protein [40]; our fluorescence images also confirm this fact [35]. Under all experimental conditions, similar images are obtained using SP-B_{1-25} and full-length SP-B (Fig. 8). This result has important implications on the design of more cost-effective replacement surfactant formulations. Currently, sources of natural SP-B from human or animal sources are limited and expensive to obtain, and a suitable expression system for the production of genetically engineered SP-B on a practical scale does not exist. Short peptide sequences are easy and cheap to synthesize and can facilitate the large scale production of replacement formulations. The elucidation of the minimal functional requirement of SP-B protein and how it relates to the amino acid sequence may allow us to design simpler and less expensive sequences which perform the same functions as SP-B.

Conclusions

An ideal replacement surfactant consists of a mixture of synthetic lipids based on those found in natural LS and synthetic protein sequences based on the LS proteins with a fully quantified mechanism of action and in vivo effect. This replacement mixture would (1) reduce the mortality rate and occurrence of BPD in nRDS infants, (2) reduce the treatment costs, and (3) provide a replacement mixture to be used in other cases of RDS such as adult RDS. We have discovered that SP-B interacts synergistically with anionic lipids such as PA to make the properties of the mixture more suitable for LS. The protein accomplishes this by acting like an emulsifying agent in the monolayer which breaks up and divides the condensed phase domains prior to collapse. This partitioning of the condensed phase shifts the mechanism of collapse from a heterogeneous, low pressure process to a homogeneous, high pressure process, and facilitates the reincorporation of collapsed phase material back into the monolayer. We have found that the amino-terminal segment of full-length SP-B, SP-B_{1-25}, captures the activity of the native protein, producing similar isotherm and morphological changes. This interaction is electrostatically based, confirmed by the reduced activity of a mutant form of SP-B_{1-25} with neutral serine residues replacing the four positively-charged residues (data not shown). The presence of the protein network may also enhance the adsorption rate of material to the interface by providing docking sites for the attachment of vesicles from the subphase.

Current and future work in our laboratory is based on studying LS on several fronts. We are trying to understand the functional mechanism of action of SP-B protein by inducing various point mutations to study the effect of varying the charge to hydrophobic balance of the protein. We are also currently engaged in studying simpler peptide sequences that capture the full activity of native SP-B. The interactions of both SP-B and SP-C with other anionic lipids found in LS, such as saturated and unsaturated phosphatidylglycerols are another area of our focus. We hope to eventually use the information gained from binary and ternary model LS systems to study a complete mixture of synthetic LS containing DPPC, anionic lipids, and synthetic protein sequences. We are also examining the mechanism of inhibition of LS by serum proteins such as albumin, an understanding of which would allow us to engineer an enhanced resistance to inhibition into these model replacement mixtures. The role chemical engineers play in surfactant research is to provide clinicians and medical researchers with novel replacement mixtures engineered for optimum performance at low cost, and to provide a complete and detailed picture of the phase behavior and properties of the mixture. Clinicians could then use this information as a basis for both designing and analyzing tests of the surfactant in animal model systems. Instead of having an extract of unknown composition with unspecified properties, clinicians would have a fully quantified system of known properties and phase behavior.

References

1. Shapiro DL, Notter RH, (eds) (1989) Surfactant Replacement Therapy. Liss, New York
2. Soll R (1992) Res Staff Phys 38:19–23
3. Kopelman AE, Mathew OP (1995) Ped Rev 16:209–217
4. Bancalari E, Sosenko I (1990) Ped Pulmon 8:109–116
5. Jobe AH (1993) New Eng J Med 328:861–868
6. Schwartz R, Anastasia M, Luby M, Scanlon J, Kellogg R (1994) New Eng J Med 330:1476–1480
7. Singh G, Yu S (1995) Am. J. Public Health 85:957–964
8. Pattle RE (1955) Nature 175: 125–1126
9. Avery ME, Mead J (1959) Am J Dis Child 97:517–523
10. Robillard E, Alarie Y, Dagenais-Perusse P, Baril E, Guilbeault A (1964) Can Med Assoc J 90:55–57
11. Enhorning G, Robertson B (1972) Pediatrics 50:55–66
12. Fujiwara T, Tanaka Y, Takei T (1980) Lancet 1:55–59
13. Possmayer F, Yu S, Weber J, Harding P (1984) Can J Biochem Cell Biol 62:1121–1131
14. Tanaka Y, Tsunetomo T, Toshimitsu A, Masuda K, Akira K, Fujiwara T (1986) J Lip Res 27:475–485
15. van Golde L, Batenburg J, Robertson B (1988) Phys Rev 68:374–455
16. Fujiwara T, Robertson B, Robertson B, Van Golde, L, Batenburg J (eds) (1992) Pharmacology of Exogenous Surfactant Elsevier, Amsterdam, pp 561–592
17. Egberts J, Sloot H, Mazure A (1989) Biochim Biophys Acta 1002:109–113
18. Yu S, Possmayer F (1992) Biochim Biophys Acta 1126:26–34
19. Pastrana-Rios B, Flach C, Brauner J, Mautone A, Mendelsohn R (1994) Biochemistry 33:5121–5127
20. Oosterlaken-Dijksterhuis M, Haagsman H, van Golde L, Demel R (1991) Biochemistry 30:8276–8281
21. Cockshutt A, Absolom D, Possmayer F (1991) Biochem Biophys Acta 1085:248–256
22. Waring, A, Taeusch W, Bruni R, Amirkhanian J, Fan B, Stevens R, Young J (1989) Pep Res 2:308–313
23. Gordon LM, Horvath S, Longo M, Zasadzinski JA, Taeusch HW, Faull K, Leung C, Waring AJ (1996) Prot Sci 5:1662–1675
24. Waring, A, Gordon L, Taeusch H, Bruni R, In: Epand R (ed) The Amphipathic Helix. CRC Press, Boca Raton, pp. 143–171
25. McConnell HM (1991) Ann Rev Phys Chem 42:171–195
26. Mobius D, Mohwald H (1991) Adv Mater 3:19–24
27. Weis R (1991) Chem Phys Lipids 57:227–239
28. Knobler CM, Desai R (1992) Ann Rev Phys Chem 43:207–264
29. Mohwald H (1993) Rep Prog Phys 56:653–685
30. Mohwald H (1990) Ann Rev Phys Chem 41:441–476
31. Riviere S, Henon S, Meunier J, Schwartz DK, Tsao MW, Knobler CM (1994) J Chem Phys 101:10045–10051
32. Schwartz D, Tsao M, Knobler C (1994) J Chem Phys 101:8258–8261
33. Henon S, Meunier J (1991) Rev Sci Instrum 62:936–939
34. Honig D, Mobius D (1991) J Phys Chem 95:4590–4592
35. Lipp MM, Lee KYC, Zasadzinski JA, Waring AJ (1996) Science 273:1196–1199
36. Chi L, Johnston R, Ringsdorf H (1991) Langmuir 7:2323–2329
37. Turnbull D (1952) J Chem Phys 20:411–432
38. Tanaka T, Ishiwata S, Ishimoto C (1977) Phys Rev Lett 38:771–774
39. Bruggeller P, Mayer E (1980) Nature 288:569–570
40. Longo ML, Bisagno A, Zasadzinski JA, Bruni R, Waring AJ (1993) Sci. 261:453–456